Magnetism of 3*d* transition-metal adatoms and dimers on graphite

D. M. Duffy and J. A. Blackman
Department of Physics, University of Reading, Whiteknights, P.O. Box 220, Reading RG6 6AF, United Kingdom
(Received 1 December 1997; revised manuscript received 3 March 1998)

The topic of this work is 3*d* transition metals deposited on a graphite surface. Spin-polarized density-functional calculations are used to obtain the magnetic moments of deposited adatoms and dimers and also their preferred position on the surface. Adatoms in the lower part of the series position themselves above C sites and their magnetic moments are higher than their free atom values, while those in the upper part display smaller moments and prefer a position above the center of a C ring. The atoms in the dimers lie either above neighboring rings or above a line through the centers of C-C bonds at opposite sides of a ring. The moments of most of the dimers are similar to their values as free diatomic molecules. Ni is nonmagnetic on the surface, both as a monomer and as a dimer. [S0163-1829(98)09935-4]

I. INTRODUCTION

Transition-metal magnetism in bulk materials is confined to five elements (Cr, Mn, Fe, Co, and Ni). The 4*d* and 5*d* elements and those in the lower part of the 3*d* series are nonmagnetic in bulk, although, as single atoms, most of the elements in the periodic table exhibit a magnetic moment. Clusters form an intermediate state between the atom and bulk, and it has been shown in molecular-beam deflection experiments[1,2] that the moments per atom of Fe, Ni, and Co are generally larger in clusters than in the bulk and approach bulk behavior at cluster sizes of a few hundred atoms. Also, nonmagnetic solids when in the form of small particles, can be magnetic converging toward atomic behavior as the size is reduced. In the 4*d* series, for example, Rh in clusters has been shown to be magnetic.[3]

The magnetism of small clusters is very sensitive to the geometry and also to the coordination of the surface sites. A review of theoretical work on the dimers of the 3*d*, 4*d*, and 5*d* elements has been given by Salahub[4] together with a comparison of experimental results. There are also a number of calculations on clusters of between 2 and 13 or so atoms: V,[5] Cr,[5–7] Co,[8,9] Fe,[7,10] Ni,[7,11] Ru,[10] Rh,[12,13] and Pd.[12]

Related observations have also been made for monolayers deposited on a surface. The moments of the ferromagnets are generally enhanced.[14] Studies of monolayers of the 4*d* and 5*d* elements on a noble-metal surface have also predicted magnetic moments. Values of $1.7\mu_B$, $1.09\mu_B$, and $0.9\mu_B$ (per atom) were obtained for Ru,[15] Rh,[16] and Ir,[17] respectively. The behavior of Os is predicted to be surface dependent,[17] being magnetic on Ag but nonmagnetic on Au. Experimental evidence for 4*d* magnetism has been reported[18] in Ru monolayers on a C(0001) surface. Calculations[19] for a C(0001) surface yield a small moment for Rh and Ru, while Pd remains nonmagnetic. The most extensive calculations for 3*d* transition-metal monolayers on graphite, the substrate of interest in the present work, are those of Krüger *et al.*[20] They consider various magnetic configurations for the elements V through Ni and compare the behavior of an epitaxially adsorbed monolayer with that of an unsupported layer.

It is also possible to form clusters on surfaces. The cluster formation can either take place on the surface itself (depositing atoms and allowing them to diffuse and aggregate) or by preforming the clusters prior to deposition. Size selection is possible with the latter technique, providing a greater uniformity in cluster size and the potential for applications. There have been a number of calculations that address the magnetic behavior of deposited 3*d*, 4*d*, and 5*d* adatoms and dimers. A Korringa-Kohn-Rostoker Green's-function technique has been used for adatoms[21,22] on Cu, Ag, Pd, Pt, and dimers on Ag.[23] Many of the atoms and dimers exhibit magnetic behavior. A particularly interesting case is that of the V_2 dimer deposited on Cu(001). Theoretical work indicates a large moment[24] that has not been detected experimentally. It has recently been shown,[25] however, that if the surface is allowed to relax, the V-V distance is similar to that in the isolated V_2 molecule and the magnetic moment is quenched.

For a graphite substrate rather little is known about the growth mode of clusters, particularly at low temperatures, and so when studying the appearance of local 3*d* magnetic moments it is necessary also to address the growth characteristics. For a single adatom, for example, one has to determine the energetically favorable position on the surface. The most detailed experiments have been done on Ag, Au, and Al,[26–29] but there has also been work[30,31] on the 3*d* transition-metals Cr, Mn, V, and Ni.

Scanning tunneling microscope measurements[26,27] indicate that single Au or Ag atoms sit above a β site (i.e., above a C atom with no atom directly below in the next layer) while Al atoms lie either above a β site or a bridge site (a C-C bond). There were no instances of atoms appearing above hole sites (centers of hexagon rings) unlike noble-gas atoms that do favor hole sites and form registered patterns. A subsequent theoretical calculation[32] is in general agreement with the behavior of Al, and our own calculations[33] on Ag are in accord with the experimental observations.

We are aware of one prior series[34,35] of calculations on transition-metal adatoms on graphite. The work, which is based on a tight-binding model, focuses on V and Cr and is partly related to an interpretation of photoemission data.[30] The authors assume that the adatoms favor a hole site. Calculations[36] have also been made for palladium-graphite interaction potentials for use in the interpretation of atomic-

force-microscopy (AFM) images of graphite.

In this paper we present first-principles electronic structure calculations for both the positions on the graphite surface and the magnetic moments of the $3d$ transition-metal elements Sc through Ni. We consider both single atoms and dimers. For the atoms we find that Fe, Co, and Ni favor hole positions while the remaining elements in the series prefer a position above C atoms. Bridge sites are never favored. In the case of dimers, the atoms prefer either neighboring holes or sites near the C-C bonds on opposite sides of a hexagon, with no systematic pattern through the series.

The magnetic moments of single atoms are generally higher than the free atom values in the lower part of the series and lower in the upper part. The moments of most of the dimers are similar to their values as free diatomic molecules. Ni is an exception and is nonmagnetic on the surface both as a monomer and a dimer. Similar behavior also occurs with a Cu(001) substrate but not for the other surfaces studied in the literature.[21]

The calculational procedure is introduced in the following section, and then the behavior of adatoms and dimers on graphite is discussed in Sections III and IV.

II. CALCULATIONAL PROCEDURE

Graphite comprises hexagonal layers of C atoms coupled by sp^2 σ bonds. The layers interact by weak van der Waals forces. To model the effect of the surface on the $3d$ adatoms or dimers, we take a finite fragment of a single C layer of appropriate symmetry; the symmetry of the cluster matches that of the local environment that the adatom or dimer would have on an infinite substrate. It is expected that the dominant interactions of the metal will be with the local carbon π orbitals. The covalent bonding within the layer is strong, so we fix the C atom separation at its value (1.42 Å) in bulk graphite. The threefold coordination of the C atoms is maintained by passivating the atoms at the edge of the cluster with H.

Checks were made that the size of fragments that are being used is sufficiently large (see Sec. III). We also tested the effect of a second layer. Changes in the binding energy are less than 0.1 eV and the presence of the second layer appears to have no effect either on the predicted moments or on the position on the surface preferred by the metal atoms. Of course, by not employing a second layer, one is not distinguishing α and β sites. That is a subtle issue, however, and is not pursued here.

The calculations were carried out using the linear combination of atomic-orbitals molecular-orbital approach within the density-functional program DMOL.[37] The exchange-correlation effects were included within the local spin-density approximation using the Vosko-Wilk-Nusair[38] parametrization. A double numeric basis set is employed augmented by polarization functions. The $3d$ core $(1s2s2p)$ electrons were frozen to speed up the calculation without affecting the accuracy of the results. As is usual, a small electronic temperature (''smearing'') was used in the calculations to accelerate convergence, but the final results correspond to zero temperature.

As an initial check on the procedure, we performed calculations for the free $3d$ dimers and for a Ag monomer on graphite for both of which there are some experimental data for comparison. We find[33] that the Ag monomer prefers a position above a C atom to a hole site in accord with experimental observation.[26,27] Using a two layer calculation, we were also able to show that it is the β site that is preferred.

The interatomic spacings of the diatomic molecules throughout the $3d$ series were calculated using both the local spin-density approximation (LSD) and gradient corrections (GC).[39,40] The interatomic separations change rather little if gradient corrections are included, and the values are in fair agreement with experiment. For example, for V we obtain values of 1.77 and 1.80 Å for LSD and GC, respectively, which compares with 1.76 Å from experiment.[41] For Cr the figures (listed in the order LSD, GC, and experiment) are 1.70, 1.81, and 1.68 Å.[42] For both of these elements, the LSD results are closer to experiment, whereas in the upper part of the series the GC is closer: Fe, 1.98, 2.02, and 2.02 Å;[43] Ni, 2.07, 2.13, and 2.16 Å.[44] The differences are small however, and they are not systematic and appear not to influence the predictions in this work, and so the LSD results are employed throughout. Further details about the free dimers including the calculated spin configurations are discussed more fully in Sec. IV.

III. ADATOMS

We describe here the calculations for single adatoms over a C atom or a hole site. In the above-atom case the layer fragment comprises the three C rings that have that atom as a common vertex and the nine rings surrounding them; there are 37 C atoms in the cluster that has C_{3v} symmetry. When the adatom is in a hole site, the six neighboring rings are used in addition to the central ring itself; there are 24 C atoms and the cluster has C_{6v} symmetry. In the LSD calculations the adatom is constrained to be above the central C atom or the center of the inner C ring, but its height is optimized to a minimum-energy configuration.

For the above-hole configuration, we checked on the effect of the cluster size by adding 12 additional rings to form a 54 C atom cluster. The change in adatom binding energy was negligible at $\sim$0.02 eV and there was no modification to the magnetic moment. It was concluded that the size of the clusters was sufficient for the current calculation. We also performed a number of calculations with an adatom above a C-C bond. There was no indication that this is ever a minimum-energy configuration for the elements considered here.

The difference in adatom binding energies between the over-hole and over-atom positions is plotted in Fig. 1. In the lower part of the series (Sc to Mn) the over-atom position is favored, while the Fe, Co, and Ni adatoms lie above the hole. The smallest energy difference occurs at $\sim$0.1 eV with Ti. This is larger than any estimated uncertainties due to the finite size of the surface cluster that has been used, and thus even for Ti one can have confidence in the identification of the preferred location of the metal atom.

The actual binding energies and vertical positions of the metal atoms are shown in Table I together with the charge and spin components. A Löwdin analysis was done to examine the contribution arising from the various atomic orbitals (a Mulliken analysis does not give significantly different re-

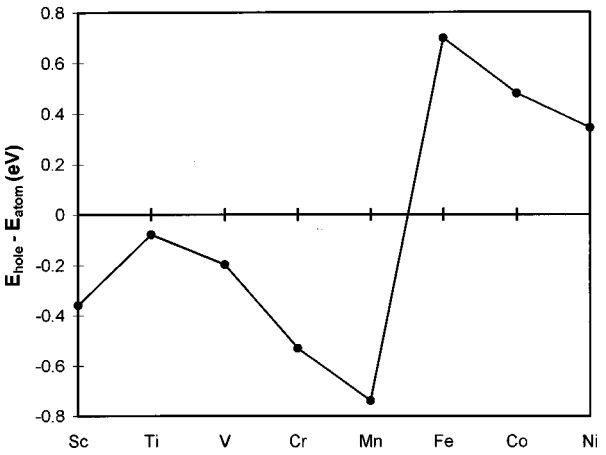

FIG. 1. Difference in binding energies (in eV) of adatoms in over-hole and over-atom positions. Positive energies mean that the over-hole site configuration is more stable.

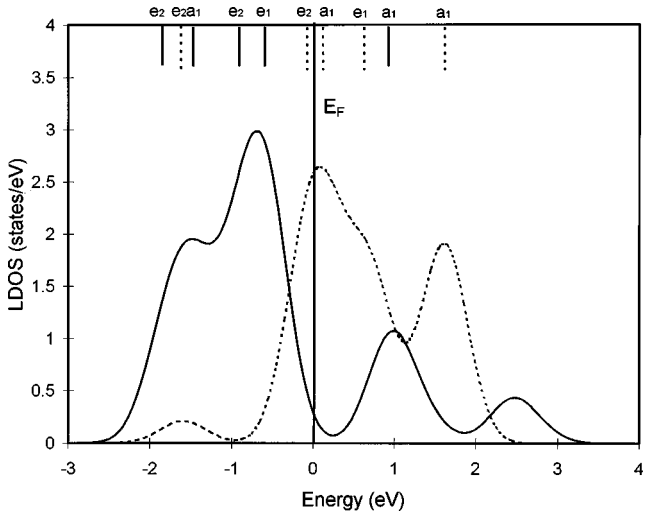

FIG. 2. Local density of states for Fe orbitals. The adatom is in the over-hole position. Gaussian broadening of the MO energy levels has been used. Energies (in eV) are with respect to the Fermi energy (taken at the center of the HOMO-LUMO gap). Principal MO energy levels with the Fe component are indicated together with symmetry label. For both LDOS and energy levels, full lines represent spin-up and broken lines spin-down.

sults). The hybridization with the π orbitals results in a small electron charge transfer to the graphite and, in the lower part of the series, a small induced moment as well. There is also some mixing from the $4p$ orbitals on the metal.

Apart from Cr, the atomic configurations of the isolated atoms are $3d^n4s^2$ where $1 \leqslant n \leqslant 8$. Cr, the exception, has $3d^5 4s^1$. The total moments in Table I are therefore higher than in the free atom by $1\mu_B$ for Sc, Ti, and V, and lower by $2\mu_B$ for Fe, Co, and Ni, while Cr and Mn have reversed their free atom values.

To understand the behavior we consider two typical elements, one (Fe) from the top part of the series and one (V) from the lower part. The spin-up and -down local density of states (LDOS) of Fe is shown in Fig. 2. It comprises mainly $3d$ and $4s$ projected orbitals with a small admixture of $4p$. The molecular orbitals (MO's) of the cluster as a whole are labeled by representations of the C_{6v} point group, namely, a_1, e_1, e_2, a_2, b_1, and b_2. Only the a_1, e_1, and e_2 orbitals have metallic as well as C π-orbital components, and the principal ones contributing to the LDOS are indicated on the figures.

The e_2 component from the $3d$ (yz and x^2-y^2) hybridizes with the π orbitals and splits into two peaks (near -1.8 and -0.9 eV for spin-up and -1.6 and -0.1 eV for spin-down). The hybridization is strong for the spin-up orbitals while of the spin-down orbitals the one at -0.1 eV has the more strongly $3d$ character. Under the peaks at -1.8 and -0.1 eV there are also a_1 components that each have about 90% $3d$ character. e_1 components having about a 70% $3d$ weighting appear under the peak at -0.6 eV and the shoulder at $+0.6$ eV. The a_1 peaks at $+0.9$ and $+1.6$ eV are about 60% $4s$.

Roughly speaking, we can say that there is a tendency, compared to the free atom, for the $4s$ levels to be shifted up in energy with respect to the $3d$. The effect is equivalent, in free atom terms, to a configuration $3d^{n+2}4s^0$ being preferred to $3d^n4s^2$. Obviously one must be careful with such a crude

TABLE I. Properties of the $3d$ adatoms. z is the height (in Å) of the adatom above the C layer, and BE is the adatom binding energy (in eV). The components of the charge and spin moment are in units of electronic charge and Bohr magnetons, respectively. The rows labeled *C* give the electronic charge transfer and the induced spin moment on the substrate. Total moment is the sum of the previous three rows. The preferred position of the adatom is noted.

	Sc	Ti	V	Cr	Mn	Fe	Co	Ni
Position	Atom	Atom	Atom	Atom	Atom	Hole	Hole	Hole
z (Å)	2.18	2.10	2.08	2.13	2.14	1.52	1.52	1.53
BE (eV)	1.9	2.1	1.6	1.0	1.0	2.0	2.4	2.5
Charge ($-e$)								
$3d$	1.5	2.6	4.0	4.8	5.4	7.2	8.2	9.2
$4sp$	1.1	1.1	0.7	0.9	1.3	0.6	0.6	0.6
C	0.4	0.3	0.3	0.3	0.3	0.2	0.2	0.2
Spin moment (μ_B)								
$3d$	1.0	2.3	3.6	4.5	4.5	1.9	1.0	0.0
$4sp$	0.9	0.7	0.5	0.7	1.1	0.1	0.0	0.0
C	0.1	0.0	-0.1	-0.2	0.4	0.0	0.0	0.0
Total moment	2	3	4	5	6	2	1	0

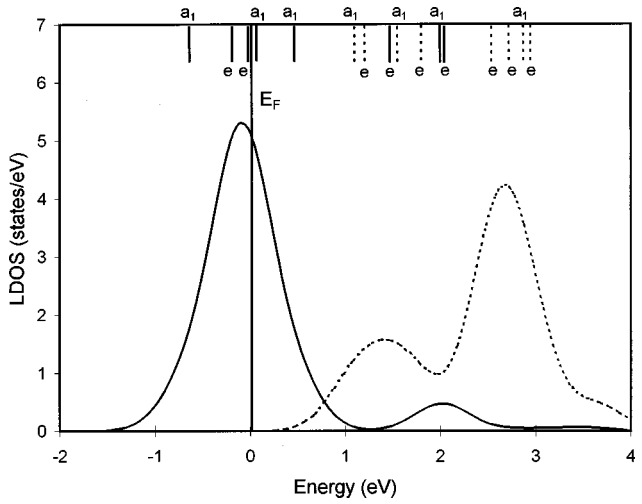

FIG. 3. Local density of states for V orbitals. The adatom is in over-atom position. Gaussian broadening of the MO energy levels has been used. Energies (in eV) are with respect to the Fermi energy (taken at the center of the HOMO-LUMO gap). Principal MO energy levels with the V component are indicated together with symmetry label. For both LDOS and energy levels, full lines represent spin-up and broken lines spin-down.

description. More accurately, the spin is maximized through the occupancy of e_1, e_2, and a_1 MO's (deriving from $3d$) while a_1 MO's (arising from $4s$) are unoccupied. However, hybridization ensures that considerable $4s$ character remains (see Table I). The discussion though does give a rough understanding of the reduction of the atomic spin moment by $2\mu_B$. Similar behavior operates with Co and Ni and leads to the absence of magnetization in the Ni adatom.

It is perhaps worth emphasizing that spurious population of $3d$ levels at the expense of the $4s$ ones, which is a feature common in LSD calculations of isolated atoms, is not a concern here. For atoms this behavior is associated with the fivefold degenerate $3d$ state and it is necessary to take into account nonsphericity to overcome the effect. Here the lower symmetry ensures that this particular problem will not arise. In fact, the enhanced $3d$ population that we are witnessing here is well known in the chemistry of carbon compounds.

We now consider V from the bottom half of the series that prefers the alternative above-atom configuration. Its local density of states is displayed in Fig. 3. The molecular orbitals of the cluster as a whole are again indicated. The labeling is by representations of the C_{3v} point group, namely a_1, e, and a_2. The a_1 and e orbitals have both metal and C π-orbital components, while a metallic component in a_2 is forbidden by symmetry. The situation is more complex here; MO levels are closer together and more orbitals from the graphite have significant hybridization. There is again a tendency for increased population of $3d$ related MO's at the expense of the $4s$. In the lower half of the series the crude argument given above would lead to an increased spin moment of $2\mu_B$. In fact, the increased hybridization reduces that effect and the increase of the spin moment from the atomic values is just $1\mu_B$.

Because we are using a finite cluster, the moments obtained have integer values. For an infinite surface, noninteger values would be possible. However, we do not expect a significant change in the values predicted here. The likelihood of such a change would occur in the instance of a small highest occupied molecular orbital-lowest unoccupied molecular orbital (HOMO-LUMO) gap with opposite spin states on either side. For the above-hole cases, Fe has the smallest such gap at 0.5 eV. In the bottom half of the Table I the smallest gap is for Sc at 0.3 eV. Neither are small enough to lead us to expect significant changes in behavior with larger substrate clusters.

The only other calculations on $3d$ transition-metal atoms on graphite that we are aware of are those of Rakotomahevitra, Demangeat, and Parlebas[34] and Krüger *et al.*,[35] which are based on tight-binding theory. They consider V and Cr and present an instructive study of the dependence of properties such as the magnetic moment on various physical parameters of the system. However, they place the atoms in a hole position whereas the present calculations indicate a preference for an above-atom position for these two elements. There is also some discrepancy between the predicted values of the equilibrium height of the atoms above the surface. They report values of 1.36 Å for V and 1.12 Å for Cr, which are significantly lower than those found here (see Table I). When the atom is constrained above a hole position we obtain values of 1.81 and 2.02 Å, respectively.

Finally in this section, it is of interest to compare the magnetic moments of adatoms on graphite with their values when on a metal substrate. Lang *et al.*[21] and Stepanyuk *et al.*[22] have performed calculations of a different type for, among other surfaces, Ag and Cu. Generally, they predict smaller moments than ours in the lower part of the series and higher ones in the upper part (by roughly $1\mu_B$ in both cases). Ni deserves special mention. The present calculations for a graphite surface yield a zero moment. Similar behavior is observed with a Cu(001) surface, but more usually (e.g., Ag, Pt, and Pd surfaces), Ni exhibits a finite moment.[21,22]

IV. DIMERS

We find that there are two possible minimum-energy configurations for a dimer placed on the surface. In the first, the atoms lie above a line joining the centers of two neighboring hexagons. The atoms are displaced either slightly outward or inward from positions vertically above the centers of the hexagons (hole sites). In the second configuration, the atoms lie above a line joining the centers of bonds on the opposite sides of a hexagon. The atoms are displaced inward slightly from positions vertically above the bond centers.

Extra C rings again surround the basic element of cluster that is necessary to define the configuration. There are 32 and 24 carbon atoms, respectively, in the two clusters. The symmetry for both situations is C_{2v} and, within the constraints of the symmetry, the atoms are free to adjust their vertical height and separation in searching for the minimum-energy position. It may be expected that if adatoms prefer to lie above C atoms, then there will be a similar tendency when the metal exists as dimers. Placed above nearest-neighbor C atoms, the interatomic separation is clearly too small. We tried starting the two metal atoms above next-nearest-neighbor C atoms, but in all cases the calculation either did not converge or the atoms moved away from their initial

TABLE II. Properties of free and supported dimers. r is the interatomic separation and z is the height above the C layer (both in Å). The components of the charge and spin moment are in units of electronic charge and Bohr magnetons, respectively. For the supported case, the rows labeled C give the electronic charge transfer and the induced spin moment on the substrate. Total moment is the sum of the appropriate rows for each case. The two columns each of Cr and Mn correspond to the antiferromagnetic (1) and full symmetry (2) configurations. The values of charge and spin are per atom. The preferred positions are noted.

		Sc	Ti	V	Cr(1)	Cr(2)	Mn(1)	Mn(2)	Fe	Co	Ni
Position		Holes	Holes	Bonds		Bonds		Holes	Bonds	Bonds	Holes
Free	r (Å)	2.22	1.92	1.77	1.70	1.62	2.49	2.53	1.98	1.95	2.07
Supp.	r (Å)	2.63	2.30	1.75		1.67		2.41	2.09	2.09	2.40
	z (Å)	1.95	1.83	2.09		2.04		1.83	1.92	1.89	1.61
Free	charge										
	$3d$	2.0	3.0	3.9	4.9	4.9	5.4	5.5	6.9	7.9	8.9
	$4sp$	1.0	1.0	1.1	1.1	1.1	1.6	1.5	1.1	1.1	1.1
	spin										
	$3d$	0	0	1.0	±2.3	0	±4.5	4.4	3.0	2.0	1.0
	$4sp$	0	0	0.0	±0.3	0	0.0	0.6	0.0	0.0	0.0
Supp.	charge										
	$3d$	1.7	2.9	4.1		5.0		5.7	6.9	7.9	9.1
	$4sp$	1.1	0.9	0.8		0.9		1.2	1.0	1.0	0.8
	C	0.2	0.2	0.1		0.1		0.1	0.1	0.1	0.1
	spin										
	$3d$	0	0	0.5		0.3		3.8	2.6	1.6	0
	$4sp$	0	0	0.3		0.5		0.4	0.4	0.4	0
	C	0	0	0.2		0.2		−0.2	0	0	0
Total moment											
	Free	0	0	1	±2.6	0	±4.5	5	3	2	1
	Supp.	0	0	1		1		4	3	2	0

position in a clear attempt to search for one of the two configurations referred to.

The minimum-energy configurations for the supported transition-metal dimers are listed in Table II. Four of the elements (Sc, Ti, Mn, and Ni) favor positions over holes, while the other four (V, Cr, Fe, and Co) prefer the bonds. The difference in bonding energies for the two configurations is shown in Fig. 4. The bonding energies are with respect to the bare substrate; they are a composite of the metal-substrate interaction and the binding energy of the dimer positioned on the substrate. It is not appropriate to compare energy with that of the free dimer because they will generally have a different interatomic spacing in the two surface configurations. The energy difference is smallest, at 0.09 eV, for the Ni dimer, but as in the previous section, possible errors in energies due to the finite substrate are smaller than the energy differences being investigated.

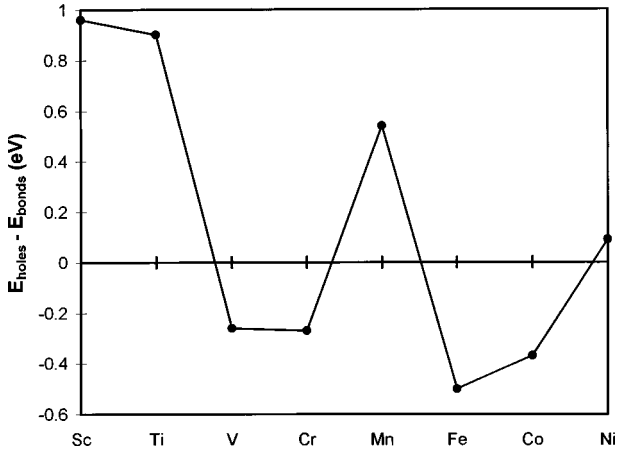

FIG. 4. Difference in binding energies (in eV) of dimers in above-holes and above-bonds positions. Positive energies mean that the above-holes configuration is more stable.

The separation of both the ring centers and the bond centers of graphite is 2.46 Å. It is convenient to discuss the behavior in the lower, middle, and upper sections of the series separately.

A. Sc, Ti, and V

Our calculations for the free diatomic molecules yield a $^1\Sigma_g^+$ ground state for Sc_2 and Ti_2 and a triplet ($\alpha\alpha$) for V_2, which are probably in agreement with the experimental situation.[4] In terms of the usual notation (irreducible representations of the $D_{\infty h}$ point group), the configurations are $\sigma_g^2\pi_u^4$, $\sigma_g^2\pi_u^4\sigma_g^2$, and $\pi_u^4\sigma_g^2\delta_g^2\sigma_g^2$ for Sc_2, Ti_2, and V_2, respectively. For the dimers on the surface, the symmetry is reduced to C_{2v}, but the ground states are unchanged from those of the free dimers in the sense that the occupied orbitals are those equivalent to the above via the compatability relations. The moments are therefore unchanged. There is some hybridization with the π orbitals and a small charge transfer to the carbon.

Sc_2 and Ti_2 show an increase in interatomic separation; for Sc_2 the separation is actually larger than the center to

center distance (2.46 Å) of neighboring C hole sites. V_2 is notable as the dimer in the series whose interatomic spacing changes least (by only 0.02 Å) when it is on the surface, and it lies well within a single ring. The strong V-V bond has been noted by Reddy, Pederson, and Khanna[25] in the context of a V_2 dimer on Cu(001). In their work, the V-V distance again remains very close to its free dimer value and relaxation of the Cu surface occurs. In our case we do not allow any surface relaxation because we expect that the covalent C bonding will keep it rather rigid. Despite this V_2 still maintains its free dimer interatomic spacing. Dimers on a Ag(001) surface have been studied by Stepanyuk *et al.*[23] They fix the V-V interatomic separations at the Ag(001) lattice spacing for both the free and supported dimer. Their assumptions are somewhat different from ours therefore, and they observe higher moments.

For these three elements then, the high spin states observed in the adatoms on graphite are no longer present. For Sc_2 and Ti_2 the moments are zero, while the V_2 molecule has a moment of $2\mu_B$ ($1\mu_B$ per atom) whether it is free or on the surface. Note that the moments in Table II are quoted per atom.

B. Cr and Mn

Cr_2 and Mn_2 are both believed to have an antiferromagnetic configuration as free dimers. However, the Cr_2 dimer is very strongly bound, while the atoms in Mn_2 are weakly coupled by a van der Waals interaction. As supported dimers, our calculations indicate a ferromagnetic configuration in both cases.

Our calculations on free Cr_2 give moments on the atoms of ± 2.6. We also obtained a Cr_2 configuration ($\pi_u^4\sigma_g^2\delta_g^4\sigma_g^2$) with full $D_{\infty h}$ symmetry and zero moment. This has a higher energy than the broken symmetry configuration but only by 0.16 eV. Both are listed in Table II [as Cr(1) and Cr(2)]. Their interatomic separations are similar at 1.70 Å for the broken symmetry configuration and 1.62 Å with full symmetry.

When on the surface the Cr-Cr separation is little changed from the free dimer value and it is very different from the lattice spacing of the surface. Like V_2, the Cr_2 dimer is strongly bound. The high stability of Cr_2 has also been noted by Cheng and Wang;[6] the dimer as a unit is apparent even when it is part of a larger chromium cluster. We were unable to obtain convergence to an antiferromagnetic configuration for the supported dimer. There is some change to the configuration when on the surface with some admixture from the C orbitals and a resultant ferromagnetic spin state of $2\mu_B$.

Mn_2 is in some ways the most problematic case. For the free molecule, we obtain an antiferromagnetic configuration that appears to relate closely to experimental observations. In particular the moment of $\pm 4.5\mu_B$ corresponds well to the full spin of $\pm\frac{5}{2}$ that is generally inferred in the interpretation of experimental data.[45,46] The molecule is weakly bound and the interatomic separation is large (although somewhat underestimated compared with experiment[45]).

In common with other authors,[47,48] we observe a number of configurations with $D_{\infty h}$ symmetry. One actually has a greater binding energy (by about 0.4 eV) than the antiferromagnetic configuration just discussed. Its occupied MO's are given by $\sigma_g^2\pi_u^3\delta_g^2\delta_u^2\sigma_g\pi_g^2\sigma_u\sigma_u$ and it has a high spin state ($5\mu_B$ per atom) and a similar Mn-Mn separation to the antiferromagnetic case. The details of both are given under Mn(1) and Mn(2) in Table II. A number of years ago there was some discussion in the literature (see Salahub's review[4]) about configurations with small interatomic separation. We also obtain such a configuration ($r=1.68$ Å) within the LSD approximation, but this becomes unbound if gradient corrections are included.

Our results for the supported Mn_2 dimer are also given in Table II. As with Cr_2, we were unable to obtain convergence to a bound antiferromagnetic configuration and the only one obtained is similar to the free Mn_2 high spin state. For the supported dimer, the $3d$ moment is somewhat reduced and there is an induced moment on the substrate that is antiparallel to that on the dimer.

C. Fe, Co, and Ni

Our calculations yield similar ground states, interatomic separations, and magnetic moments to other recent work[8–10,12] for free Fe_2, Co_2, and Ni_2 molecules with configurations $\sigma_g^2\pi_u^4\delta_g^3\delta_u^2\sigma_g^2\pi_g^2\sigma_u$, $\sigma_g^2\pi_u^4\sigma_g^2\delta_g^4\sigma_u\pi_g^2\delta_u^3$, and $\sigma_g^2\pi_u^4\sigma_g^2\delta_g^4\sigma_u^2\pi_g^2\delta_u^4$, respectively. Both Fe_2 and Co_2 change rather little on the surface. The magnetic moment of each matches its free dimer values though there is some shifting of the components from $3d$ to $4s/4p$. There is an increase in interatomic spacing of a little over 0.1 Å but it is still well short of a graphite lattice spacing.

The effect of the surface is stronger with Ni_2. There is a big increase in interatomic spacing and $r=2.40$ Å falls only a little short of the distance between C ring centers (2.46 Å). Also the moment of $2\mu_B$ on the molecule vanishes when it is placed on the surface. An understanding of this can be reached following the discussion under the adatoms (Sec. III) where we referred to a tendency to push $4s$ levels up in energy in comparison with the $3d$ ones. Effectively what happens is that the electrons in the filled σ_g^2 orbital in free Ni_2 move to the partially filled π_g^2 orbital resulting in a configuration of $\pi_u^4\sigma_g^2\delta_g^4\sigma_u^2\pi_g^4\delta_u^4$ for the dimer on the surface. The earlier comments about hybridization and using orbital labels related through the compatibility relations obviously applies here as well.

V. CONCLUSIONS

The purpose of this work is twofold: to investigate the preferred positions of $3d$ transition-metal atoms and dimers on a graphite surface, and to examine their magnetic behavior.

The positions of the adatoms show a clear trend, lying above sites up to Mn in the series and over rings for Fe, Co, and Ni. The dimers favor one of two possible configurations also but, unlike the single atom case, no systematic trend develops.

We examined the magnetic moment for the two adatom positions. For an atom above a ring, the pattern discussed for Fe persists throughout the series (viz., a decrease/increase by $2\mu_B$ from the free atom value in the top/bottom part of the series). When positioned above a C atom the pattern described for V persists and, instead, the decrease/increase is

by $1\mu_B$. Ni is a special case and exhibits zero moment in whichever position it is placed. It is also nonmagnetic as a dimer, and we have also observed the same behavior in groups of three and four Ni atoms confined to the surface. It will be interesting to see if an incipient three-dimensional structure is a necessary condition for a finite spin. A similar zero moment is also observed[20] with a Cu(001) substrate. Apart from Ni as just mentioned and Cr and Mn, which are special cases, there is a strong tendency for the dimers to maintain the magnetic behavior shown as free molecules.

There has been some experimental work[26,27,30] on the morphology of small metallic clusters on graphite and their growth as two- or three-dimensional objects. A feature emerging from the present work is the rather little change in the free dimer interatomic spacing when placed on the surface—particularly for V, Cr, Fe, and Co. This contrasts with Ni, which is much more flexible in attempting to match the graphite lattice spacing. It will be interesting to investigate how this behavior develops as the size of the clusters is increased. There is likely to be a considerable variety of growth characteristics across the 3*d* series. Such contrasting behavior has already been observed in preliminary molecular dynamics studies[49] on Ni, which prefers two-dimensional growth while its neighbor Cu exhibits a three-dimensional behavior.

ACKNOWLEDGMENT

One of us (D.M.D.) acknowledges the support of the Daphne Jackson Memorial Fellowships Trust.

[1] I. M. L. Billas, A. Châtelain, and W. A. de Heer, Science **265**, 1682 (1994).
[2] J. P. Bucher, D. C. Douglas, and L. A. Bloomfield, Phys. Rev. Lett. **66**, 3052 (1991); J. P. Bucher and L. A. Bloomfield, Int. J. Mod. Phys. B **7**, 1079 (1993).
[3] A. J. Cox, J. G. Louderback, and L. A. Bloomfield, Phys. Rev. Lett. **71**, 923 (1993).
[4] D. R. Salahub, in *Ab Initio Methods in Quantum Chemistry II*, edited by K. P. Lawley (John Wiley, Chichester, 1987), p. 447.
[5] K. Y. Lee and J. Callaway, Phys. Rev. B **49**, 13 906 (1994).
[6] H. Cheng and L.-S. Wang, Phys. Rev. Lett. **77**, 51 (1996).
[7] G. M. Pastor, J. Dorantes Dávila, and K. H. Bennemann, Phys. Rev. B **40**, 7642 (1989).
[8] C. Jamorski, A. Martinez, M. Castro, and D. R. Salahub, Phys. Rev. B **55**, 10 905 (1997).
[9] Z. Q. Li and B. L. Gu, Phys. Rev. B **47**, 13 611 (1993).
[10] M. Castro and D. R. Salahub, Phys. Rev. B **49**, 11 842 (1994).
[11] F. A. Reuse and S. N. Khanna, Chem. Phys. Lett. **234**, 77 (1995).
[12] B. V. Reddy, S. N. Khanna, and B. I. Dunlap, Phys. Rev. Lett. **70**, 3323 (1993).
[13] P. Villaseñor González, J. Dorantes Dávila, H. Dreyssé, and G. M. Pastor, Phys. Rev. B **55**, 15 084 (1997).
[14] C. L. Fu, A. J. Freeman, and T. Oguchi, Phys. Rev. Lett. **54**, 2700 (1985).
[15] S. Blügel, Europhys. Lett. **18**, 257 (1992).
[16] M. J. Zhu, D. M. Bylander, and L. Kleinman, Phys. Rev. B **43**, 4007 (1991).
[17] S. Blügel, Phys. Rev. Lett. **68**, 851 (1992).
[18] R. Pfandzeller, G. Steierl, and C. Rau, Phys. Rev. Lett. **74**, 3467 (1995).
[19] L. J. Chen, R. Q. Wu, N. Kioussis, and J. R. Blanco, J. Appl. Phys. **81**, 4161 (1997).
[20] P. Krüger, A. Rakotomahevitra, J. C. Parlebas, and C. Demangeat, Phys. Rev. B **57**, 5276 (1998).
[21] P. Lang, V. S. Stepanyuk, K. Wildberger, R. Zeller, and P. H. Dederichs, Solid State Commun. **92**, 755 (1994).
[22] V. S. Stepanyuk, W. Hergert, K. Wildberger, R. Zeller, and P. H. Dederichs, Phys. Rev. B **53**, 2121 (1996).
[23] V. S. Stepanyuk, W. Hergert, P. Rennert, K. Wildberger, R. Zeller, and P. H. Dederichs, Phys. Rev. B **54**, 14 121 (1996).
[24] H. Nait-Laziz, C. Demangeat, and A. Mokrani, J. Magn. Magn. Mater. **121**, 123 (1993).
[25] B. V. Reddy, M. R. Pederson, and S. N. Khanna, Phys. Rev. B **55**, R7414 (1997).
[26] E. Ganz, K. Sattler, and J. Clarke, Surf. Sci. **219**, 33 (1989).
[27] G. M. Francis, I. M. Goldby, L. Kuipers, B. von Issendorff, and R. E. Palmer, J. Chem. Soc. Dalton Trans. **5**, 665 (1996).
[28] V. Maurice and P. Marcus, Surf. Sci. **275**, 65 (1992).
[29] Q. Ma and R. A. Rosenberg, Surf. Sci. **391**, L1224 (1997).
[30] C. Binns, S. H. Baker, A. M. Keen, S. N. Mozley, C. Norris, H. S. Derbyshire, and S. C. Bayliss, Phys. Rev. B **53**, 7451 (1996).
[31] M. Bäumer, J. Libuda, and H.-J. Freund, Surf. Sci. **327**, 321 (1995).
[32] I. Moullet, Surf. Sci. **331-333**, 697 (1995).
[33] D. M. Duffy and J. A. Blackman, Surf. Sci. (to be published).
[34] A. Rakotomahevitra, C. Demangeat, and J. C. Parlebas, J. Phys.: Condens. Matter **6**, 3321 (1994).
[35] P. Krüger, M. Taguchi, J. C. Parlebas, and A. Kotani, Phys. Rev. B **55**, 16 466 (1997).
[36] D. Tomanek and W. Zhong, Phys. Rev. B **43**, 12 623 (1991).
[37] DMOL, version 4.0.0, Molecular Simulations, San Diego, CA, 1996.
[38] S. H. Vosko, L. Wilk, and M. Nusair, Can. J. Phys. **58**, 1200 (1980).
[39] A. D. Becke, J. Chem. Phys. **88**, 2547 (1988).
[40] J. P. Perdew and Y. Wang, Phys. Rev. B **45**, 13 244 (1992).
[41] P. R. R. Langridge-Smith, M. D. Morse, G. P. Hansen, R. E. Smalley, and A. J. Merer, J. Chem. Phys. **80**, 593 (1984).
[42] S. M. Casey and D. G. Leopold, J. Phys. Chem. **97**, 816 (1993).
[43] H. Purdum, P. A. Montano, G. K. Shenoy, and T. Morrison, Phys. Rev. B **25**, 4412 (1982).
[44] J. Ho, M. L. Polak, K. M. Erwin, and W. C. Lineberger, J. Chem. Phys. **99**, 8542 (1986).
[45] C. A. Baumann, R. J. VanZee, S. V. Bhat, and W. Weltner, J. Chem. Phys. **78**, 190 (1983).
[46] M. Cheeseman, R. J. Van Zee, H. L. Flanagan, and W. Weltner, J. Chem. Phys. **92**, 1553 (1990).
[47] D. R. Salahub and N. A. Baykara, Surf. Sci. **156**, 605 (1985).
[48] J. Piechota and M. Suffczynski, Int. J. Mod. Phys. B **7**, 560 (1993).
[49] D. M. Duffy, J. A. Blackman, P. A. Mulheran, and S. A. Williams, J. Magn. Magn. Mater. **177-181**, 953 (1998).